12^{th} International Conference on Fracture Mechanics of Concrete and Concrete Structures
FraMCoS-12
B.L.A. Pichler, Ch. Hellmich, P. Preinstorfer (Eds)

https://doi.org/10.21012/FC12.1276
MS05-1:1

AN ELASTOPLASTIC PHASE FIELD MODEL FOR FRACTURE IN CONCRETE BASED ON A GENERALIZED CONTINUUM FORMULATION

SINA ABRARI VAJARI[*], MATTHIAS NEUNER[†] AND CHRISTIAN LINDER[‡]

[*] Department of Civil and Environmental Engineering, Stanford University
Stanford, CA, USA
e-mail: abrari@stanford.edu

[†] Institute of Structural Engineering, University of Natural Resources and Life Sciences
Vienna, Austria
e-mail: matthias.neuner@boku.ac.at

[‡] Department of Civil and Environmental Engineering, Stanford University
Stanford, CA, USA
e-mail: linder@stanford.edu

Key words: Phase Field Fracture, Concrete, Elastoplastic, Mixed Mode Fracture, Generalized Continuum

Abstract. Concrete's complex heterogeneous internal structure leads to an involved quasi-brittle response where a progressive loss of material integrity is observed. Additionally, in real-life applications, concrete structures are under loading conditions resulting in complex mixed-mode fracture patterns. Hence, prediction of crack behavior in concrete structures is a challenging task. Owing to the high costs of experimental testing, computational modeling has emerged as a viable alternative for studying concrete fracture. The phase field approach has proven to be a well-established formulation for simulating different fracture phenomena, where crack propagation is tracked implicitly using an additional independent field that diffuses the damage. Previously we introduced a phase field model investigating various crack driving forces considering only the elastic response of concrete. Following a thermodynamically consistent approach, we extend that model to an elastoplastic formulation which can accurately capture the quasi-brittle response of concrete, including the pressure dependency of strength. We formulate the equations within a generalized continuum framework, which accounts for the microstructure of the solid, naturally captures the size effect of materials, and addresses stability issues arising from complex plastic formulations. We demonstrate that employing this framework captures the internal microstructure of concrete by incorporating an internal length scale, which characterizes the microstructural fracture response and represents the finite size of the fracture process zone ahead of the crack tip. A comparison with experimental results confirms the good performance of the model in capturing mixed-mode I-II or I-III failures of concrete.

1 INTRODUCTION

The prediction of fracture nucleation and propagation, one of the most prevalent failure mechanisms, is critically important for engineering applications to prevent catastrophic structural failures. Among construction materials, concrete exhibits a complex fracture behavior due to its heterogeneous composition of cement mortar and grains. This heterogeneity gives rise to a quasi-brittle response, where material integrity deteriorates gradually rather than the abrupt loss of load-carrying capacity observed in brittle materials. Additonaly, in practical engineering, concrete structures are frequently subjected to loading conditions that produce complex mixed-mode fractures, such as mode I-II (combined opening and sliding) or mode I-III (combined opening and tearing) patterns [1]. Consequently, predicting failure in concrete structures presents a considerable challenge.

Owing to the high costs of experimental testing, computational modeling has emerged as a viable alternative for studying concrete fracture. Among the various fracture modeling techniques, the phase field approach has gained significant attraction over the past two decades due to its inherent ability to simulate crack nucleation, propagation, and bifurcation without requiring ad hoc criteria. In phase field models, the crack surface evolution is described implicitly via an order parameter (the crack phase field), which transitions smoothly between intact and fully cracked states. This approach contrasts with discrete crack models, where cracks are explicitly represented by introducing displacement discontinuities into the kinematic descriptions [2–4].

The phase field method in mechanics was pioneered by Francfort and Marigo [5], who developed it based on the variational formulation of Griffith's theory for brittle fracture [6]. Later, Bourdin et al. [7] introduced a numerical implementation by regularizing the formulation with a length scale parameter. Since then, the phase field approach has been extensively developed and applied to a range of failure mechanisms, including brittle fracture [8, 9], ductile fracture [10, 11], and fracture in polymers [12, 13].

Most phase field models primarily address the brittle behavior of solids, with only a limited number focusing on the quasi-brittle failure commonly observed in concrete. Among these, an even smaller subset addresses mixed-mode fracture of concrete [14, 15].

To address this gap, we first present our thermodynamically consistent phase field model tailored for the quasi-brittle fracture of concrete [16]. The model, with a focus on capturing mixed-mode failure patterns, features a straightforward formulation that implicitly integrates various failure conditions within the framework by deriving crack driving forces based on widely used failure criteria. Specifically, these criteria are incorporated into the governing equations through equivalent effective stress measures that account for the stress state. This approach captures the pressure-dependent strength and the asymmetric response of concrete under tensile and compressive loads. A general form of the equivalent effective stress measure is proposed to unify the formulation, enabling straightforward implementation into a finite element framework. This unified approach not only facilitates the incorporation of diverse failure criteria into the model but also enables a systematic comparison of their performance in predicting mixed-mode fracture in concrete. Such comparisons are crucial, as different failure criteria yield varying responses under identical loading conditions.

Next, we extend that model to an elastoplastic formulation which can accurately capture the quasi-brittle response of concrete. We formulate the equations within a generalized continuum framework, which accounts for the microstructure of the solid, naturally captures the size effect of materials, and addresses stability issues arising from complex plastic formulations. This framework can capture the internal microstructure of concrete by incorporating an internal length scale, which characterizes the microstructural fracture response and represents the finite size of the fracture process zone ahead of the crack tip. A comparison with experimental results also confirms the good performance of the model in capturing mixed-mode I-II or I-III failures of concrete.

The outline of the paper is as follows. Section 2 introduces a purely geometric approach to damage modeling, where an evolution equation equates the rate of crack formation with the power of a crack driving force. In this section, a unified formulation of the equivalent effective stress measure is proposed, capturing a range of failure criteria. Section 3 extends the model to an elastoplastic micropolar continuum, providing a robust framework to accurately represent the quasi-brittle behavior of concrete while accounting for concrete's microstructure. Section 4 presents simulations of mixed-mode fracture in concrete, including a comparison of numerical load–displacement curves and predicted crack paths against experimental data. Finally, conclusions are summarized in Section 5.

2 GENERALIZED DRIVING FORCE FOR THE DAMAGE FIELD

2.1 Phase field approximation

To model the evolution of cracks within a continuum, a time-dependent parameter $d \in [0,1]$, referred to as the crack phase field, is introduced. This parameter differentiates between an intact material point ($d = 0$) and a fully damaged one ($d = 1$). Based on the physical principle that cracks evolve irreversibly, the phase field satisfies the constraint $\dot{d} \geq 0$.

The introduction of the crack phase field enables the representation of a sharp crack surface using a diffuse (regularized) approximation [8, 17], expressed as

$$\int_{\mathcal{S}} \mathrm{d}\mathcal{S} \approx \int_{V} \Gamma \, \mathrm{d}V \,, \tag{1}$$

where Γ is the crack surface density function [18]. This function is defined in terms of the crack phase field d, its gradient $d_{,i}$, and the phase field length scale l_{d}

$$\Gamma(d, d_{,i}; l_{\mathrm{d}}) = \frac{1}{c_0} \left(\frac{1}{l_{\mathrm{d}}} w(d) + l_{\mathrm{d}} \, d_{,i} \, d_{,i} \right) . \tag{2}$$

Here, $w(d)$ is the geometric crack function, which governs the homogeneous and local evolution of the crack phase field [19], while l_{d} acts as a regularization parameter controlling the width of the diffuse crack. The parameter c_0 serves as a scaling factor, ensuring convergence to a sharp crack surface as l_{d} approaches zero [19].

2.2 Phase field equation

For the crack evolution equation, the purely geometric approach outlined in [20, 21] is employed. An evolution equation that equalizes the rate of crack formation with the power of a crack driving force is postulated in the form

$$\frac{\mathrm{d}}{\mathrm{d}t} \left(\int_V \Gamma \, \mathrm{d}V \right) = \mathcal{H} \left(d, \dot{d}, \mathcal{Y} \right) . \tag{3}$$

In this equation, $\mathcal{H}$ is a crack driving functional depending on the crack phase field, its rate, and a local crack driving force $\mathcal{Y}$ that accounts for the history of the solid. As discussed in [20], this general equation allows for different driving forces to affect the evolution of damage, enriching the framework to account for various phenomena such as brittle cracking, ductile fracture, or asymmetric fracture responses in tension and compression, which are important characteristics for modeling quasi-brittle materials like concrete.

Similar to [20], we write the crack driving functional in (3) as a power expression in the form

$$\mathcal{H} \left(d, \dot{d}, \mathcal{Y} \right) = \frac{1}{G_{\mathrm{c}}} \int_V \left(-g'(d) \mathcal{Y} - \mathcal{R} \right) \dot{d} \, \mathrm{d}V \,, \tag{4}$$

where $\mathcal{R}$ is a function of $\dot{d}$, accounting for the viscous crack resistance effects, and G_{c} is the critical fracture energy, a material parameter reflecting the resistance of the body to cracking. Furthermore, $g'(d) = \frac{\mathrm{d}g}{\mathrm{d}d}$ denotes the derivative of the degradation function $g(d)$ with respect to the crack phase field d. The degradation function, reflects the dependency of the strain energy on the phase field parameter and models the loss of stiffness with the evolution of damage.

After some calculations, the global crack surface evolution equation, induces a local equation in the form

$$\frac{2 \, G_{\mathrm{c}}}{c_0} \, l_{\mathrm{d}} \, d_{,ii} = \frac{G_{\mathrm{c}}}{c_0 \, l_{\mathrm{d}}} w' + g' \mathcal{Y} \,. \tag{5}$$

2.3 Constitutive relations

Following [19], the crack surface density function Γ and the degradation function g are chosen such that, in the 1D case, for a vanishing phase field length scale parameter l_{d}, the resulting mode I behavior of the framework is equivalent to a cohesive zone model, allowing for the incorporation of different softening laws.

Hence, geometric crack function to the form

$$w(d) = 2d - d^2 \,, \tag{6}$$

and a degradation function in the general form

$$g(d) = \frac{(1-d)^p}{(1-d)^p + Q(d)} \,, \tag{7}$$

with

$$Q(d) = b_1\, d \left(1 + b_2\, d + b_2\, b_3\, d^2\right) > 0 \,, \tag{8}$$

are used. Considering the Cornelissen [22] softening law for normal concrete, the optimal calibrated parameters are given as [19]

$$\begin{aligned} p &= 2, \quad b_1 = \frac{4}{\pi\, l_{\mathrm{d}}} \frac{E\, G_{\mathrm{c}}}{f_{\mathrm{t}}^2}, \\ b_2 &= 1.3868, \quad b_3 = 0.6567 \,, \end{aligned} \tag{9}$$

with E as the Young's modulus and f_{t} as the tensile strength.

Following the common phase field formulations [8], the local crack driving force can be taken as

$$\mathcal{Y} = \Psi^{\mathrm{e}} \,. \tag{10}$$

This indicates that the damage is driven by the entire elastic strain energy Ψ^{e}, with no distinction between different energy contributions. Accordingly, the proposed model does not differentiate between the tensile and compressive contributions of Ψ^{e}. As a result, the formulation leads to symmetric fracture responses under both tensile and compressive loads. However, this behavior might not be realistic for quasi-brittle materials such as concrete, where the compressive strength is an order of magnitude higher than the tensile strength.

To address this issue, various decompositions of the strain energy have been introduced in phase-field fracture models. For instance, Amor et al. [23] proposed a spherical and deviatoric decomposition of the strain energy, and Miehe et al. [18] developed a mechanism to differentiate crack responses under tensile and compressive loads based on the spectral decomposition of the strain tensor.

Although phase field formulations based on these energy decompositions effectively predict the fracture response of concrete, they often involve complex models that require explicit consideration of various cracking modes [24, 25]. Accordingly, a more advanced driving force inspired by the works of [19, 26] on quasi-brittle materials, is assumed as

$$\mathcal{Y} = \frac{1}{2E} \left\langle \bar{\sigma}_{\mathrm{eq}} \right\rangle^2 \,, \tag{11}$$

with $\bar{\sigma}_{\mathrm{eq}}$ as the equivalent effective stress, a scalar quantity that accounts for the stress state at a material point. The incorporation of the equivalent effective stress provides a simple yet effective framework capable of capturing the complex fracture response of concrete and driving the evolution of damage accordingly.

Following our previous work [16], the equivalent effective stress is written as

$$\begin{aligned} \bar{\sigma}_{\mathrm{eq}} =& c_1\, \rho\, r\,(\theta, e) + c_2\, \zeta + \\ & \sqrt{\left(c_1\, \rho\, r\,(\theta, e) + c_2\, \zeta\right)^2 + c_3\, \rho^2} \,, \end{aligned} \tag{12}$$

where ζ is the hydrostatic stress invariant, ρ is the deviatoric stress invariant, θ is the deviatoric polar angle, e is the eccentricity parameter that describes the out-of-roundness of the deviatoric trace, and r defines the shape of the yield surface in the deviatoric section [27]. Moreover, c_1, c_2, and c_3 are constants given in Table 1, required to derive specific equivalent effective stresses based on the Rankine, Drucker-Prager, modified von Mises, and the three-parameter failure criteria.

This generalization not only facilitates a straightforward implementation into a finite element framework but also offers flexibility in selecting the appropriate driving force for a given experiment being simulated. For instance, if the structure undergoes tension-dominated failure, the Rankine equivalent effective stress may be an appropriate choice. However, in scenarios where the compressive strength of concrete plays a significant role, an alternative driving force should be selected to accurately capture the material's behavior.

Table 1: Parameters of the generalized form (12) for deriving specific equivalent effective stress measures. In these equations, the parameter $k = f_c/f_t$ is the ratio of the compressive strength f_c to the tensile one f_t.

Equivalent effective stress	c_1	c_2	c_3
Rankine	$\frac{1}{2\sqrt{6}}$	$\frac{1}{2\sqrt{3}}$	0
Drucker-Prager	$\sqrt{\frac{3}{8}}\frac{k+1}{2k}$	$\frac{\sqrt{3}}{4}\frac{k-1}{k}$	0
Modified von Mises	0	$\frac{\sqrt{3}}{2}\frac{k-1}{k}$	$\frac{3}{2k}$
Three-parameter	$\frac{\sqrt{3}\left(k^2-1\right)e}{2\sqrt{2}k^2(e+1)}$	$\frac{\sqrt{3}\left(k^2-1\right)e}{2k^2(e+1)}$	$\frac{3}{2k^2}$

3 EXTENSION TO GENERALIZED CONTINUA

So far the material behavior of concrete was modeled within an elastic framework, capturing the onset and propagation of cracks effectively for certain applications. However, concrete exhibits a complex mechanical response that includes significant inelastic deformations and microstructural effects, particularly under high-stress conditions or in post-peak regimes. To address these limitations, we aim to extend our formulation to include plasticity and account for the microstructure of concrete. For this purpose, we employ a generalized continuum formulation, specifically the micropolar theory [28].

The micropolar formulation offers several advantages for modeling quasi-brittle materials like concrete. It introduces additional degrees of freedom, such as rotations of microelements, and incorporates couple stresses, which enable the simulation of microstructural effects that cannot be captured by classical continuum theories. This approach is particularly beneficial for describing phenomena such as strain localization, which is heavily influenced by the internal structure of the material, and for mitigating mesh sensitivity issues in numerical simulations.

A micropolar continuum represents a continuous collection of material points, where each material point is defined by a displacement field u_i, as well as an additional microrotation vector ϕ_i. This microrotation field characterizes the local rotation of material points and is considered an independent kinematic variable.

To extend the formulations defined in the previous section, we use the generalized strain measures. In a micropolar continuum, the strain tensor ε_{ij} is computed using both the displacement field and the microrotation field, given by

$$\varepsilon_{ij} = u_{j,i} + \epsilon_{jik}\phi_k \, , \tag{13}$$

where ϵ_{jik} is the Levi-Civita permutation symbol. Additionally, the spatial gradient of the microrotation field defines the wryness tensor γ_{ij} as

$$\gamma_{ij} = \phi_{i,j} \, . \tag{14}$$

To incorporate the plastic response of concrete, we adopt the formulation presented in [29], with its extension to a micropolar framework described in [30]. This approach accounts for the non-symmetry of the stress tensor and the presence of couple stresses.

For the phase-field formulation, we follow the approach presented in [20], where a geometric crack function $w = d^2$ and a degradation function $g = (1-d)^2$ are used. Moreover, the power expression defined in Equation (4) is reformulated as

$$\mathcal{H} = \frac{1}{l_\mathrm{d}} \int_V ((1-d)\,\mathcal{Y})\,\dot{d}\,\mathrm{d}V\,. \qquad (15)$$

For the micropolar formulation, we introduce the local crack driving force as

$$\mathcal{Y} = \begin{cases} 0 & \text{if } \alpha_\mathrm{p} < 1 \\ \mathcal{E}\alpha_\mathrm{p} & \text{if } \alpha_\mathrm{p} \geq 1\,, \end{cases} \qquad (16)$$

with α_p as the internal plastic variable. As for $\mathcal{E}$, it is a parameter related to the fracture energy of concrete G_c, and is calibrated based on the area under the load-displacement curve for a mode-I test.

This specific form indicates that, in a micropolar continuum (under tension-dominated cases), damage is primarily driven by plastic deformation.

4 NUMERICAL SIMULATIONS

To validate the proposed phase field model, we conduct a numerical study of an experimental test focusing on the mixed-mode fracture of concrete. First, we present the results using the classical elastic formulation outlined in Section 2, followed by the same example analyzed using the micropolar extension introduced in Section 3.

4.1 Single-edge notched specimen using the classical formulation

We examine a single-edge notched concrete beam subjected to an antisymmetric four-point loading configuration using the classical elastic formulation. As illustrated in figure 1, the beam measures 440 mm × 100 mm × 100 mm and features a vertical notch measuring 5 mm × 20 mm × 100 mm at the top center. Experimentally observed by Schlangen [31], this loading setup produces a curved crack path that initiates at the right corner of the notch and propagates to the right edge of the lower-right loading platen.

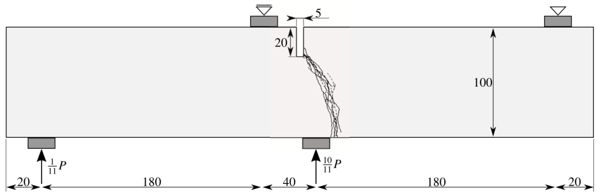

Figure 1: Geometry (in mm) and boundary conditions of the single-edge notched beam, with the experimental crack paths.

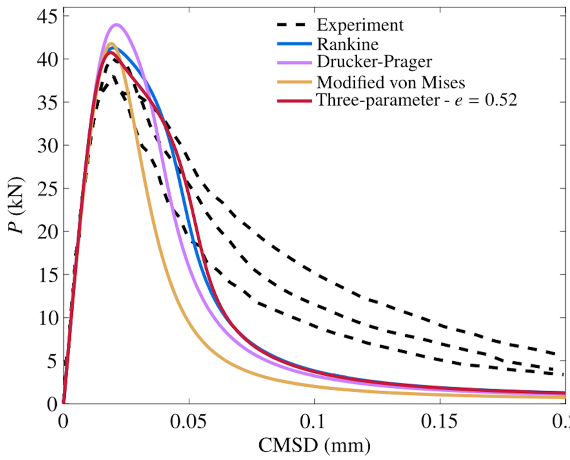

Figure 2: Computed and experimental load–CMSD curves for the single-edge notched beam example using various equivalent effective stresses.

For the numerical simulation, to reduce computational costs, the specimen is modeled as a 3D body with a thickness of 5 mm and discretized using 8-node brick elements. The element size is set to 0.6 mm in regions where crack propagation is expected. The loading and support platens are represented as steel plates. The load P is applied using an indirect displacement control technique, monitoring the Crack Mouth Sliding Displacement (CMSD), defined as the relative vertical displacement between the notch faces at the top of the beam. For the material parameters used refer to [16].

The predicted load-CMSD curves obtained with each equivalent effective stress measure, along with the experimental data, are shown in figure 2. A good agreement is observed between the simulated and experimental results, particularly in capturing the peak load for all stress measures. However, the post-peak behavior is underestimated in all cases, with the simulated load-carrying capacity degrading faster and reaching its final value earlier than observed experimentally.

The evolution of the crack phase field for each equivalent effective stress measure is illustrated in figure 3. In all cases, the crack initiates at the notch tip and propagates downwards towards the lower-right loading plate, consistent with experimental observations.

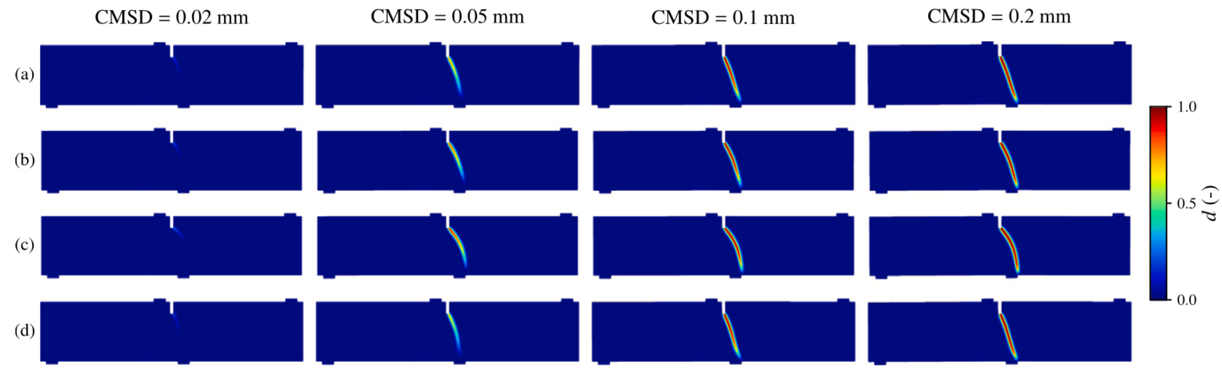

Figure 3: Evolution of damage using the (a) Rankine, (b) Drucker–Prager, (c) modified von Mises, and (d) three-parameter equivalent effective stresses.

4.2 Single-edge notched specimen using the micropolar formulation

Now, we examine the same example using the micropolar formulation. For the additional material parameter, the value of parameter $\mathcal{E}$ used in equation (16) was calibrated based on $G_c = 0.12$ N/mm and is equal to 0.0011.

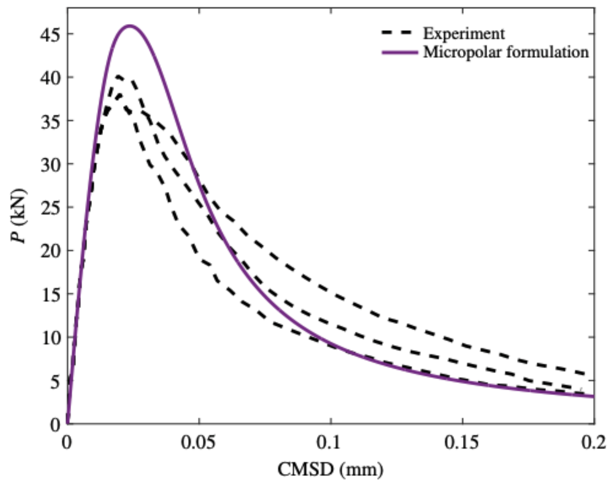

Figure 4: Computed and experimental load–CMSD curves using the micropolar formulation.

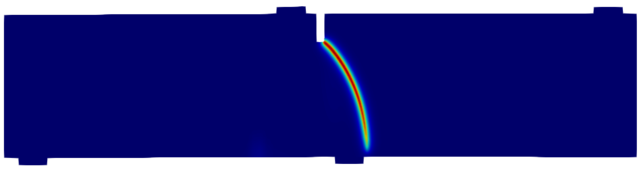

Figure 5: Final crack path using the micropolar formulation.

Figures 4 and 5 present the predicted load-CMSD curves and the predicted crack path, respectively. A good agreement between the experimental observations and the simulated results is observed.

We observe that using a micropolar elastoplastic model with a simpler geometric crack function $w = d^2$ and degradation function $g = (1-d)^2$, instead of the more complex counterparts shown in equations (6) and (7) required in our previous work, yields good results.

5 Conclusion

This work proposed a phase field framework for predicting the quasi-brittle cracking of concrete, with a particular focus on mixed-mode failure patterns. Starting from thermodynamic principles, a geometric approach to fracture was adopted, introducing an evolution equation that balances the rate of crack formation with the power of an arbitrary crack-driving force.

As shown in our previous work, the crack driving force was linked to an equivalent effective stress measure, a scalar quantity that accounts for the stress state at material points. This approach enabled the implicit incorporation of various failure conditions. By deriving different equivalent effective stress measures from a unified general form, the model accounted for common failure criteria. This generalization not only simplified finite element implementation but also provided the flexibility to select appropriate driving forces for specific applications.

To further enhance the model and address additional complexities in concrete behavior, such as microstructural effects and plasticity, we extended the formulation to a micropolar continuum framework. Our observations highlighted that combining a concrete plasticity model with a simpler degradation function could produce accurate results.

The proposed framework was validated through examples showcasing mixed-mode cracking patterns in concrete. The results demonstrated the model's ability to effectively capture the complex mixed-mode cracking behavior of concrete, confirming its robustness and applicability.

Acknowledgments

Financial support for this research was provided by the Department of Energy, National Nuclear Security Administration, Predictive Science Academic Alliance Program (PSAAP) under Award Number DE-NA0003962. This support is gratefully acknowledged.

References

[1] Zhi-Min Wu, Rena C. Yu, Chang-Yu Sun, Yan-Jie Wang, Xiao-Xin Zhang, and Xiao-Dong Fei. A new test method for the complete load-displacement curve of concrete under mixed mode i-ii fracture. *Theoretical and Applied Fracture Mechanics*, 108:102629, 2020.

[2] Nicolas Moës, John Dolbow, and Ted Belytschko. A finite element method for crack growth without remeshing. *International journal for numerical methods in engineering*, 46(1):131–150, 1999.

[3] C. Linder and F. Armero. Finite elements with embedded strong discontinuities for the modeling of failure in solids. *International Journal for Numerical Methods in Engineering*, 72(12):1391–1433, 2007.

[4] Francisco Armero and Christian Linder. New finite elements with embedded strong discontinuities in the finite deformation range. *Computer Methods in Applied Mechanics and Engineering*, 197:3138–3170, 2008.

[5] Gilles A Francfort and J-J Marigo. Revisiting brittle fracture as an energy minimization problem. *Journal of the Mechanics and Physics of Solids*, 46(8):1319–1342, 1998.

[6] Alan Arnold Griffith. The phenomena of rupture and flow in solids. *Philosophical transactions of the royal society of London. Series A*, 221(582-593):163–198, 1921.

[7] B. Bourdin, G.A. Francfort, and J-J. Marigo. Numerical experiments in revisited brittle fracture. *Journal of the Mechanics and Physics of Solids*, 48(4):797–826, 2000.

[8] Christian Miehe, Fabian Welschinger, and Martina Hofacker. Thermodynamically consistent phase-field models of fracture: Variational principles and multi-field fe implementations. *International journal for numerical methods in engineering*, 83(10):1273–1311, 2010.

[9] Marreddy Ambati, Tymofiy Gerasimov, and Laura De Lorenzis. A review on phase-field models of brittle fracture and a new fast hybrid formulation. *Computational Mechanics*, 55(2):383–405, Feb 2015.

[10] M. Ambati, T. Gerasimov, and L. De Lorenzis. Phase-field modeling of ductile fracture. *Computational Mechanics*, 55(5):1017–1040, 2015.

[11] Sina Abrari Vajari, Matthias Neuner, Prajwal Kammardi Arunachala, Andy Ziccarelli, Gregory Deierlein, and Christian Linder. A thermodynamically consistent finite strain phase field approach to ductile fracture considering multi-axial stress states. *Computer Methods in Applied Mechanics and Engineering*, 400:115467, 2022.

[12] Prajwal Kammardi Arunachala, Sina Abrari Vajari, Matthias Neuner, Jay Sejin Sim, Renee Zhao, and Christian Linder. A multiscale anisotropic polymer network model coupled with phase field fracture. *International Journal for Numerical Methods in Engineering*, 125(13):e7488, 2024.

[13] Prajwal Kammardi Arunachala, Sina Abrari Vajari, Matthias Neuner, and Christian Linder. A multiscale phase field fracture approach based on the non-affine microsphere model for rubber-like materials. *Computer Methods in Applied Mechanics and Engineering*, 410:115982, 2023.

[14] Jian-Ying Wu, Yuli Huang, Hao Zhou, and Vinh Phu Nguyen. Three-dimensional phase-field modeling of mode i + ii/iii failure in solids. *Computer Methods in Applied Mechanics and Engineering*, 373:113537, 2021.

[15] De-Cheng Feng and Jian-Ying Wu. Phase-field regularized cohesive zone model (czm) and size effect of concrete. *Engineering Fracture Mechanics*, 197:66–79, 2018.

[16] Sina Abrari Vajari, Matthias Neuner, Prajwal Kammardi Arunachala, and Christian Linder. Investigation of driving forces in a phase field approach to mixed mode fracture of concrete. *Computer Methods in Applied Mechanics and Engineering*, 417:116404, 2023.

[17] Blaise Bourdin, Gilles A Francfort, and Jean-Jacques Marigo. The variational approach to fracture. *Journal of elasticity*, 91(1-3):5–148, 2008.

[18] Christian Miehe, Martina Hofacker, and Fabian Welschinger. A phase field model for rate-independent crack propagation: Robust algorithmic implementation based on operator splits. *Computer Methods in Applied Mechanics and Engineering*, 199(45-48):2765–2778, 2010.

[19] Jian-Ying Wu. A unified phase-field theory for the mechanics of damage and quasi-brittle failure. *Journal of the Mechanics and Physics of Solids*, 103:72–99, 2017.

[20] Christian Miehe, Lisa-Marie Schänzel, and Heike Ulmer. Phase field modeling of fracture in multi-physics problems. part i. balance of crack surface and failure criteria for brittle crack propagation in thermo-elastic solids. *Computer Methods in Applied Mechanics and Engineering*, 294:449–485, 2015.

[21] C. Miehe, M. Hofacker, L.-M. Schänzel, and F. Aldakheel. Phase field modeling of fracture in multi-physics problems. part ii. coupled brittle-to-ductile failure criteria and crack propagation in thermo-elastic–plastic solids. *Computer Methods in Applied Mechanics and Engineering*, 294:486–522, 2015.

[22] H Cornelissen, D Hordijk, and H Reinhardt. Experimental determination of crack softening characteristics of normalweight and lightweight concrete. *Heron*, 31(2):45–46, 1986.

[23] Hanen Amor, Jean-Jacques Marigo, and Corrado Maurini. Regularized formulation of the variational brittle fracture with unilateral contact: Numerical experiments. *Journal of the Mechanics and Physics of Solids*, 57(8):1209–1229, 2009.

[24] Ye Feng, Jiadi Fan, and Jie Li. Endowing explicit cohesive laws to the phase-field fracture theory. *Journal of the Mechanics and Physics of Solids*, 152:104464, 2021.

[25] Ye Feng and Jie Li. Phase-field method with additional dissipation force for mixed-mode cohesive fracture. *Journal of the Mechanics and Physics of Solids*, 159:104693, 2022.

[26] Jian-Ying Wu. A geometrically regularized gradient-damage model with energetic equivalence. *Computer Methods in Applied Mechanics and Engineering*, 328:612–637, 2018.

[27] K. Willam and E. Warnke. Constitutive models for the triaxial behavior of concrete. In *Proceedings of the International Association for Bridge and Structural Engineering*, volume 19, pages 1–30, Bergamo, Italy, 1975.

[28] A Cemal Eringen. *Microcontinuum field theories: I. Foundations and solids*. Springer Science & Business Media, 2012.

[29] Peter Grassl and Milan Jirásek. Damage-plastic model for concrete failure. *International Journal of Solids and Structures*, 43(22):7166–7196, 2006.

[30] M. Neuner, S. Abrari Vajari, P.K. Arunachala, and C. Linder. A better understanding of the mechanics of borehole breakout utilizing a finite strain gradient-enhanced micropolar continuum model. *Computers and Geotechnics*, 153:105064, 2023.

[31] H.E.J.G. Schlangen. *Experimental and numerical analysis of fracture processes in concrete*. PhD thesis, Delft University of Technology, 1993.